RESEARCH ARTICLE

Laser Deposited Nanostructured Thin Film Catalyst of Cobalt Oxide for Hydrogen Generation

H. Jadhav[1,2,*] and S. Sinha[1,3]

[1]Laser & Plasma Surface Processing Section, Bhabha Atomic Research Centre, Trombay, Mumbai 400085, India
[2]Department of Physics, University of Mumbai, Vidyanagari, Santacruz (East), Mumbai 400098, India
[3]Homi Bhabha National Institute, Anushaktinagar, Mumbai 400094, India

*Corresponding author: E-mail: jadhav.hs2013@gmail.com

DOI: 10.5185/amlett.2021.011594

Thin film with immobilized particulates of Cobalt oxide (Co_3O_4) has been synthesized by Pulsed Laser Deposition (PLD) technique followed by thermal treatment in air. Surface morphology of the Co_3O_4 films was examined using Field Emission Scanning Electron Microscopy (FESEM). Crystalline structure of Co_3O_4 films was investigated by X-ray Diffraction (XRD) and Raman spectroscopy was used to confirm the presence of Co_3O_4 phase on the surface. Efficient catalytic performance was obtained with these films for hydrolysis in Sodium Borohydride ($NaBH_4$). A maximum hydrogen generation rate of ~5100 mL min^{-1} g^{-1} of catalyst was recorded at a temperature of 305 K with calculated activation energy of 62.96 kJ/mol. Good catalytic activity could be attributed to nanostructures of the films formed following heat treatment consisting of densely packed nanoparticles (NPs) which act as active catalytic centers, and the immobilized nature of the particles on the surface of the films. These catalyst films showed no major loss of activity even after five cycles of use allowing at the same time an advantage of easy separation from the solution. Our results thus demonstrate good catalytic performance and reusability of such PLD deposited Co_3O_4 nanostructured films towards hydrogen production by hydrolysis of $NaBH_4$.

Introduction

Hydrogen (H_2) is emerging as a promising energy carrier due to its high energy content and zero emission of greenhouse gases. Chemical hydrides are attractive H_2 storing materials for portable applications. Among these hydrides, Sodium borohydride ($NaBH_4$) has received considerable attention due to its high H_2 content (10.8 wt %), chemical stability, low cost and potentially safe operation [**1**]. Hydrolysis of $NaBH_4$ in presence of non-noble catalyst is a widely accepted method for H_2 production since it is a cleaner route of generating H_2 under moderate conditions. Non-noble metal catalyst systems have displayed good catalytic performance for hydrolysis [**1-2**]. Among these, Co-based materials have been largely investigated as cost-effective catalysts to accelerate hydrolysis of $NaBH_4$ with good catalytic activity [**3**].

Various Co-based materials such as, Co-B, Co-P and Co-Ni have been widely studied as efficient catalysts for hydrolysis reactions [**4-6**]. Catalytic activity of Co-B powder and Pulsed laser deposited (PLD) Co-B films for hydrolysis of $NaBH_4$ have been reported in [**2**]. Effect of laser and process parameters such as, laser fluence and distance between substrate and target, respectively, on the properties of deposited Co-B films is reported in detailed along with catalytic activity study [**2**]. Different nanostructures of Co oxide including nanoparticles (NPs) [**7**], nanorods [**8**], macrocubes [**9**] and core shell nanowires [**10**] have also been studied for $NaBH_4$ hydrolysis with favorable catalytic performance. Extensive efforts have been made to improve catalytic performance of Co-based materials by using various synthesis methods. Particle agglomeration during catalytic reactions is a major issue while using catalyst in the form of powder. Agglomeration of NPs not only decreases their catalytic performance, but also makes their recycling performance very poor. Keeping particles separated during the course of reaction becomes highly difficult in powder catalyst, thus gradually decreasing their catalytic activity with time. To overcome the problem of agglomeration, catalytic particles have been dispersed or supported on substrates like porous materials and commercial foams [**11-12**]. Co- nanocrystal assembled hollow NPs have been reported as active and robust catalyst and Co supported on honeycomb matrix has also been employed for the hydrolysis reactions [**13**]. Although many approaches have been applied to improve performance of the catalyst, it still remains a great challenge to design catalysts having immobilized active sites spread over large surface area avoiding at the same time agglomeration of catalyst particles without any support.

Catalyst in the form of a thin film is a good solution to overcome the problems associated with powder catalyst. Thin film catalysts prevent particle agglomeration owing to the immobilized nature of the catalyst particles on the surface of the film. Also, such thin film catalysts can be easily recovered and reused over several runs. In particular, coatings of assembled nanoparticles (NPs) provide high surface area and good stability against agglomeration owing to their immobilized state and adherence to substrate. Thin film catalysts have been

prepared by various chemical and physical deposition methods such as, electroless plating [**14**], magnetic field induced chemical reduction method [**15**], magnetron sputtering [**16**] and pulsed laser deposition (PLD) [**2**]. However, synthesis of nanostructures on the coating surface with desired size and morphology along with advantageous physical and chemical properties is still a difficult task to achieve. Among different deposition techniques Pulsed laser Deposition (PLD) stands out as a unique technique on account of its many advantages over others, mainly precise control over almost all the deposition parameters. Effect of various deposition parameters (such as laser fluence, distance between target and substrate) on the catalytic activity of the PLD deposited Co-B thin film catalyst has been reported in [**2**]. Effect of post heat treatment in air on PLD deposited Co-B thin films (deposited on Si substrate) were also explored in [**17**]. A complete 3D urchin like microstructure was formed when the Co-B film was annealed in air at 600^0C for 8 hours. Microstructural as well as compositional (decomposition of Co-B phase) changes in the Co-B film when annealed in air at temperatures ranging from 400-600^0C were systematically studied and reported in [**17**]. These 3D urchin structured Co_3O_4 films (deposited on Si) were used as thin planar cathodes for field emission applications [**17**]. PLD deposited Co_3O_4 films were used as thin planar cold cathodes for field emission applications and also used as thin film catalysts for H2 producing reactions [**17,24**].

In present work we report synthesis and catalytic activity of Co_3O_4 nanostructured thin film catalyst deposited on glass substrate by PLD in vacuum and followed by thermal treatment in air. Field Emission Scanning Electron Microscopy (FESEM) has been used to study morphological evolution of the nanostructured assembled thin films. X-ray Diffraction (XRD) measurement was carried out to study the crystalline structure of these films. Catalytic activity of Co_3O_4 thin films towards H_2 production by hydrolysis of $NaBH_4$ has been studied systematically. Our study establishes good catalytic performance of such PLD based Co_3O_4 thin films post heat treatment demonstrating a maximum hydrogen generation rate of ~5100 ml^{-1} min^{-1} g^{-1} of catalyst with good reusability.

Experimental

Cobalt boride (Co-B) powder was synthesized using chemical reduction method as reported in [**2**]. Co-B powder was used as starting material (not Co or CO_3O_4) for the deposition. Co-B powder was chosen based on our previous study in which we have observed that B plays an important role in the formation of nanostructured thin films after heat treatment [**17**]. Similar growth of nanostructures was not observed when we annealed pure Co film deposited by PLD for identical annealing conditions. Co-B powder of 1.5 gm was cold pressed at a pressure of ~1500 kg/cm^2 to form a circular disc of 25 mm diameter with a thickness of ~ 3-4 mm and used as a target material for laser ablation. Surface roughened glass slides were used as substrates to deposit Co-B coatings, surface roughening being done to enhance adhesion of coating with substrate. Simultaneously, deposition was carried out on silicon substrates for the purpose of characterization. In order to obtain uniform ablation of the target with minimum change in its surface geometry the Co-B target was mounted on a rotating target holder, while the substrate was kept fixed on a substrate holder. Deposition of Co-B films was carried out using a pulsed Nd-YAG laser operating at a wavelength of 532 nm, pulse duration of 5 ns and repetition rate of 10 Hz. The PLD chamber was evacuated up to a base pressure of 10^{-5} mbar. All PLD runs were carried out at room temperature and at a fixed distance of ~ 4 cm between Co-B target and substrates. Laser fluence (20 J/cm^2) and distance between target and substrate (4 cm) were optimized. The Co-B target was irradiated using 30000 laser pulses and number of pulses was kept constant for all PLD runs. Weight of the thin film catalyst (1 mg) was calculated by measuring the weight of the glass slide before deposition and after deposition. Subsequent to laser deposition, these Co-B thin films were annealed in air at temperature of 600^0C with a heating rate of 10^0C/min for duration of 8 hours. The annealing temperature and duration period were selected based on our previous work reported in [**17**]. These heat-treated thin films were tested as catalysts for hydrolysis reaction.

Surface morphology of films was studied using Field Emission Scanning Electron Microscopy (FESEM). Crystalline phase of the films was determined by X-ray diffractometer with Cu Kα radiation (λ=1.5414 A^0). Grazing incidence XRD (GIXRD) measurements were performed at room temperature at a grazing angle of incidence of 0.8^0. XRD measurements were performed over the 2θ range of 30^0-70^0 with data collected at a scanning speed of 2^0/min. Raman spectral characterization of these thin films was performed with excitation wavelength of 532 nm, laser power of 8.5 mW, over a spectral range of 100–2000 cm^{-1} with spectral resolution of 1 cm^{-1}.

An alkaline stabilized solution of $NaBH_4$ and NaOH (0.025 ±0.001 M) was prepared for catalytic activity measurements. NaOH was added into the solution to avoid self-hydrolysis of $NaBH_4$. 100 ml of the above solution was used for each catalytic activity measurement. Catalyst in the form of thin films was kept in the reaction chamber and then aqueous solution of $NaBH_4$ was added to it under continuous stirring at 305 K. Before hydrolysis measurements these Co_3O_4 heat treated catalytic films were activated in 1 wt% $NaBH_4$ solution for ~30 minutes and then loaded in the reaction chamber to carry out hydrolysis reaction. H_2 volume generated by hydrolysis reaction was measured using gas volumetric method. Detailed description of the measurement apparatus used in this study is reported in [**18**]. Weight of the catalyst deposited in form of coating was 1 mg and kept same for each activity run.

Results and discussion

Fig. 1(a) shows FESEM image of as deposited Co-B film synthesized by PLD. Spherical particulates with wide size distribution in the range of few nm to 1-2 µm were observed on the surface of film. Such morphology of the films deposited using PLD technique can be explained by phase explosion phenomena which occurs at sufficiently high laser fluence [**2**]. **Fig. 1(b)** shows SEM image of Co-B film prepared by PLD followed by thermal treatment in air at a temperature of 600^{0}C for 8 hours. The spherical particulates of Co-B have been observed to be deformed due to heat treatment in air. These deformed particles have many smaller particles of nm size on the surface. Numerous small particles protruding from surface and radially distributed on surface of spherical particles of 1µm size are clearly evident in **Fig. 1(c)**. Deformation of the PLD deposited particles with numerous small particles protruding outwards on heat treatment can be attributed to stress induced growth mechanism [**17**]. These particles (Fig. 1c) are expected to act as active catalytic centers for the catalytic reactions of hydrogen generation due to their higher surface area as compared to the spherical smooth particles (Fig. 1a).

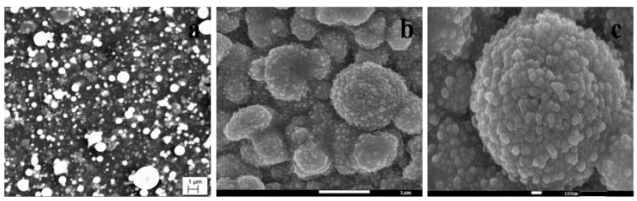

Fig. 1. FESEM images of (a) Co-B film deposited by PLD, (b) Co-B film heat treated in air at 600^{0}C for 8 hours and (c) single Co-B particle after heat treatment in air at 600^{0}C for 8 hours.

Amorphous nature of the as deposited Co-B films was confirmed as reported in [**2**]. **Fig. 2** shows XRD spectra of PLD deposited Co-B film annealed at 600^{0}C for 8 hrs in air. The peaks centered at 2θ = 31.4^0, 36.9^0, 44.8^0, 59.4^0 and 65.4^0 are assigned to the cubic structure of Co_3O_4 as acquired from JCPDS data file 76-1802. These diffraction peaks correspond to the (220), (311), (400), (511) and (440) planes respectively. Additional peaks detected at 2θ = 42.5^0 and 61.6^0 indicates the presence of CoO phase according to JCPDS file 78-0431.The diffraction peak appearing at 2θ=51.5^0 (marked by # in **Fig. 2**) is attributed to silicon substrate. To calculate crystallites size, two prominent peaks corresponding to reflections from (311) and (400) planes have been considered. Crystallites size calculated using Scherrer's equation was found to lie in the range of 10-12 nm. No signature of boron or boron oxide was detected in the XRD spectra of the film after annealing at 600^{0}C for 8 hours in air. This confirms that the film is mainly composed of Co_3O_4 phase subsequent to heat treatment in air. Edla et al. also reported formation of Co_3O_4 phase when Co-B films were heat treated at 600^{0}C for 4 hrs in air **[19]**. Decomposition of Co-B phase has been observed for annealing above 400^{0}C in air [**19**].

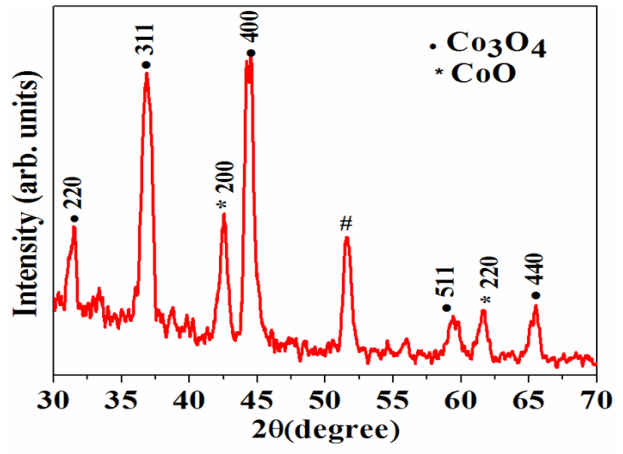

Fig. 2. XRD spectra of Co-B film annealed at 600^{0}C for 8 hrs in air.

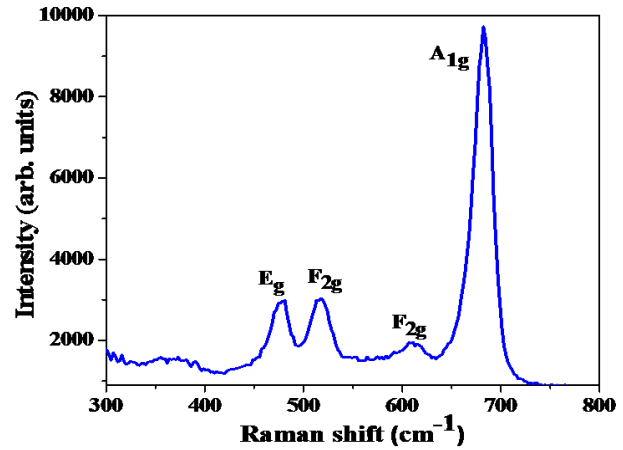

Fig. 3. Raman spectra of Co-B film heat treated at 600^{0}C for 8 hrs in air.

Fig. 3 shows Raman spectra recorded for the post deposition annealed film having Co_3O_4 nanostructure. The peaks centered at 477, 517, 611 and 682 cm^{-1} corresponds to the various vibration modes of crystalline Co_3O_4. The peak at 517 and 611 cm^{-1} are associated with F_{2g} symmetry. The band at 477 cm^{-1} is assigned to E_g symmetry. The strong band at 682 cm^{-1} is attributed to A_{1g} symmetry which corresponds to the octahedral sites of crystalline Co_3O_4 phase [**20**].

Hydrolysis reaction of 100 ml 0.025 M $NaBH_4$ in presence of Co_3O_4 thin film catalysts was carried out at a temperature of 305 K. **Fig. 4** shows the graph of H_2 production yield as a function of time. NaOH was added to $NaBH_4$ solution to inhibit self-hydrolysis. As shown in **Fig. 4** the Co_3O_4 catalyst film was able to produce H_2 instantaneously as soon as it came in contact with $NaBH_4$ solution without induction period to initiate hydrolysis reaction. This could be because of the prior activation of the film in $NaBH_4$ solution. Nanostructured heat treated PLD deposited film was able to generate 100% H_2 in 100 minutes (**Fig. 4**). Catalytic activity measured in terms of hydrogen generation rate (HGR) exhibited by the Co_3O_4 films was compared with other nanostructures of Co oxide and these results are presented in **Table 1**.

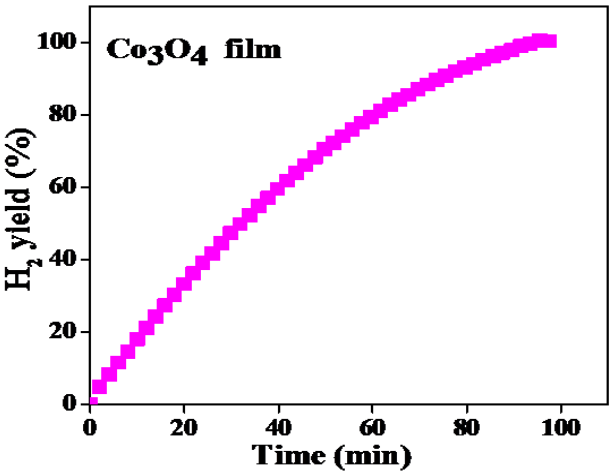

Fig. 4. Hydrogen production yield as a function of time exhibited by PLD deposited Co_3O_4 film.

Table 1. Comparison of various Co-based catalysts used for $NaBH_4$ hydrolysis.

Sr. No.	Catalyst used	Temperature (^{0}C)	HGR (mL min^{-1} g^{-1} of catalyst)	Ref.
1	Commercial Co_3O_4 powder	25	900	21
2	Co_3O_4 nanorods	25	1940	5
3	Co NPs_ 3D GO particles	25	4394	10
4	Co_3O_4macrocubes	25	1498	9
5	Co NPs_C2N matrix	30	8930	22
6	ALD Co_3O_4 film	30	3250	23
7	PLD Co_3O_4 film	30	5010	24
8	PLD annealed film	32	5100	Present study

Maximum H_2 generation rate (HGR) of ~5100mL min^{-1} g^{-1} of catalyst was measured for Co_3O_4 nanostructured films in our study. Our present catalyst when compared with other nanostructures was observed to be largely superior in terms of HGR (**Table 1**). Catalytic performance of our samples was higher than that obtained from commercial Co_3O_4 powder (900 mL min^{-1} g^{-1} of catalyst) [**21**]. Array of Co_3O_4 nanorods supported on Ti sheet was able to achieve maximum HGR of 1940 mL min^{-1} g^{-1} of catalyst [**5**]. Highly dispersed Co oxide NPs supported on 3D graphene oxide particles generated H_2 at a rate of 4394 mL min^{-1} g^{-1} of catalyst [**10**] whereas, 1498 mL min^{-1} g^{-1} HGR is reported for Co_3O_4 macrocubes synthesized by hydrothermal synthesis [**8**]. Only Co oxide nanoparticles embedded in C2N polymer structure displayed higher HGR of 8930 mL min^{-1} g^{-1} of catalyst than our present catalyst [**22**]. Co_3O_4 film deposited by atomic layer deposition (ALD) also showed lower rate of ~3250 mL min^{-1} g^{-1} of catalyst [**23**] when compared to present catalyst, while, Co_3O_4 film deposited by PLD at 250^{0}C substrate deposition temperature [**24**] exhibits nearly comparable H_2 rate as our present thin film catalyst.PLD is a potential method for deposition of nanoparticles embedded thin films of various catalytic materials [**2**]. Well separated and immobilized nanoparticles were observed on the surface of film (Fig. 1) deposited using PLD. These NPs acts as active sites for catalytic reactions. Size and density of these NPs can be varied in a controlled manner by changing PLD parameters such as, laser fluence, laser wavelength and distance between substrate and target. Catalytic performance of thin film catalysts depends critically on particle size and density. Increment in HGR was recorded for film deposited by PLD and post heat treated in air. This increased HGR is attributed to the change in morphology after heat treatment.

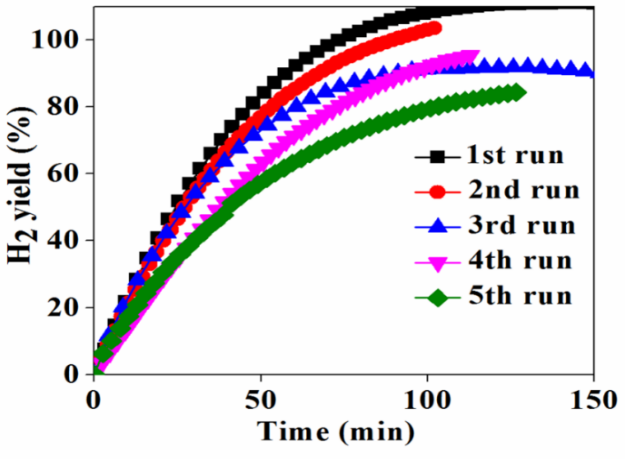

Fig. 5. Reusability test of Co_3O_4 nanostructured film.

It is always important to determine reusability of the developed catalyst for its commercial applications. The as prepared Co_3O_4 nanostructured catalyst was tested for its reusability by recycling the catalyst for a total of 5 runs using 100 ml of 0.025 M $NaBH_4$ solution at a temperature of 305 K. After each run the catalyst was taken out and washed in distilled water. Measured H_2 generation yield, as a function of time for number of hydrolysis runs is shown in **Fig 5**. The test results of the present catalyst show that after second run the H_2 yield reduces by ~10%, whereas, after fourth run a reduction in H_2 yield of ~20% was recorded. The observed reduction could have occurred on account of mass loss of Co_3O_4 film as indicated by observed minor peeling of the coating at isolated spots during the process of hydrolysis. Thus, from the observed results it is clear that the present catalyst exhibits good reusability and stability both of which are of great importance for practical applications.

The hydrolysis reaction data was further investigated to obtain activation energy (E_a) for the hydrolysis of $NaBH_4$ catalyzed by Co_3O_4 nanostructured films. For this the hydrolysis reactions were performed at varied temperatures ranging from 302 to 315 K (**Fig. 6(a)**). The HGR increased with increase in temperature as observed from **Fig. 6(a)**, from 3350 mL min^{-1} g^{-1} Co_3O_4 at 302 K to 9800 mL min^{-1} g^{-1} Co_3O_4 at 315 K. This increase in HGR can be attributed to the accelerated movement of the $NaBH_4$ molecules due to increased reaction temperature,

which leads to increasing effective collisions of the $NaBH_4$ molecules. E_a was determined according to Arrhenius equation stated as follows,

$$\ln k = \ln (A) - (E_a/RT) \quad (1)$$

Here k is the HGR (mL min^{-1} g^{-1} Co_3O_4), T is the reaction temperature, A is the pre-exponential factor and R is gas constant (8.314 J/K/mol). Slope of the Arrhenius plot **Fig. 6(b)** of ln (HGR) versus 1/T was used to calculate the E_a of nanostructured Co_3O_4 catalyzed $NaBH_4$ reaction which was determined to be ~62.96 kJ/mol. This value compares well with other Co_3O_4 nanostructures [**5,9**].

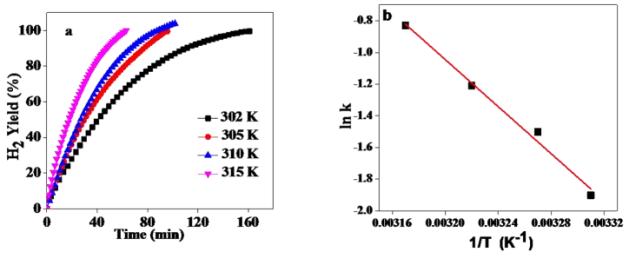

Fig. 6. (a) hydrogen generation rate influenced by temperature in the presence of Co_3O_4 thin film catalyst and (b) the corresponding Arrhenius plot.

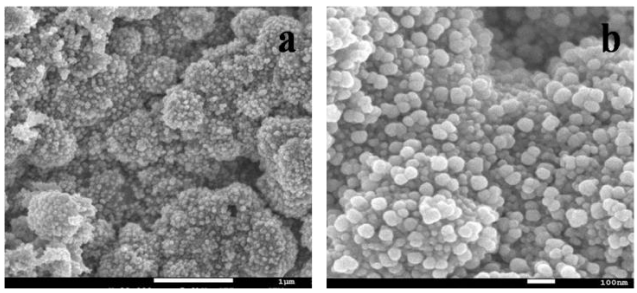

Fig. 7. FESEM images of Co_3O_4 thin film catalyst after hydrolysis runs.

Fig. 7 shows typical FESEM images of our Co_3O_4 NPs assembled thin film catalyst after their use in hydrolysis reaction. That the assembly of Co_3O_4 nanostructures is well maintained even after the hydrolysis reaction is evident in **Fig. 7**. This immobilized and maintained nanostructure of the thin film catalyst allows the catalyst to be effective for several hydrolysis runs without major loss of catalytic activity. This property in particular, exhibited by these thin film catalysts could make them the preferred catalyst of choice for commercial applications.

In order to determine structural changes if any, that may occur in the catalytic thin film after repeated use in hydrolysis reaction, XRD spectra of Co_3O_4 thin film catalyst was recorded and compared before and after use in hydrolysis reactions. This is presented in **Fig. 8**. Comparison of XRD patterns of Co_3O_4 before and after participating in the catalytic process demonstrates that Co_3O_4 still remains the main component of catalyst after the hydrolysis reaction. In addition, it can be seen that CoO peaks which were present in the film have disappeared after the hydrolysis reaction and two minor peaks centered at 38.6º and 55.8º (marked as*) have appeared which correspond to the Co_xB active phase [**25**]. The absence of CoO phase after hydrolysis reaction suggests that CoO could have been transformed either, into Co or Co_xB phase. These observations are in agreement with results which report that Co_3O_4 gets partially transformed into Co_xB phase during hydrolysis reaction [**6**].

Our FESEM and XRD results of the Co_3O_4 films before and after hydrolysis reactions demonstrate good stability of the films in terms of morphology and structure for the hydrogen evolution reactions. Good stability and efficient hydrogen generation rate make such type of Co_3O_4 thin film catalysts cost effective, as well as, durable for commercial applications on a large scale.

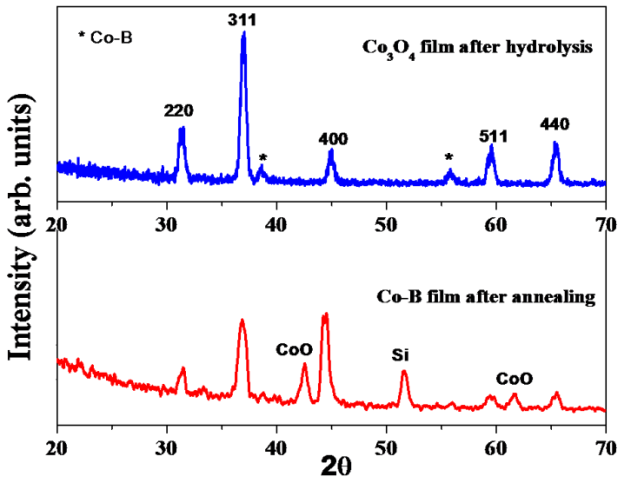

Fig. 8. Comparison of XRD spectra of Co-B thin film catalyst after annealing and Co_3O_4 film after hydrolysis process.

Conclusion

Nanostructured Co_3O_4 films were synthesized by PLD followed by thermal treatment in air. Morphological study reveals well grown nanoparticles on the surface of the film after annealing at 600^0C in air. The mechanism responsible for growth of nanofeatures protruding on surface in outward direction can be attributed to stress induced growth process. The obtained Co_3O_4 films are crystalline in nature. Catalytic tests demonstrate that such catalyst shows good performance with a maximum hydrogen generation rate of ~5100 mL min^{-1} g^{-1} of catalyst. Moreover, the present catalyst exhibits excellent reusability during the catalytic process. Our results thus confirm that Co_3O_4 thin film catalyst deposited by PLD technique and heat treated performs as an efficient catalyst for the hydrolysis of $NaBH_4$. Morphological and structural analysis of Co_3O_4 thin films catalyst after hydrolysis process demonstrates good stability.

Acknowledgement

This work was supported by collaboration PhD program between University of Mumbai and Bhabha Atomic Research Centre, Mumbai, India. Authors gratefully acknowledge Dr. S Basu, BARC for experimental support provided for X-ray diffraction measurements. S. Sinha acknowledges receiving Raja Ramanna Fellowship from DAE, India.

Keywords

Immobilized nanostructures, hydrogen production, pulsed laser deposition

Received: 30 April 2020
Revised: 25 May 2020
Accepted: 01 September 2020

References

1. Brack, P.; Dann, S.; Wijayantha, K.; *Energy Sci. Eng.*, **2015**, *3*, 174.
2. Jadhav, H.; Singh, A.K.; Patel, N.; Fernandes, R.; Gupta, S.; Kothari, D.C.; Miotello, A.; Sinha, S.; *Appl. Surf. Sci.*, **2016**, *387*,358.
3. Patel, N.; Miotello, A.; *Int. J. Hydrogen Energy*, **2015**, *40*, 1429.
4. Wan, Z.; Xu, Q.; Li, H.; Zhang, Y.; Ding, Y.; Wang, J.; *Appl. Catal. B- Environ.*, **2017,** *210*, 67.
5. Mondschein, J.; Callejas, J.; Read, C.; Chen, J.; Holder, C.; Badding, C.; Schaak, R.; *J. Chem. Mater.*, **2017**, *29*, 950.
6. Huang, Y.; Wang, K.; Cui, L.; Zhu, W.; Asiri, A.; Sun, X.; *Catal. Commun.*, **2016,** *87*, 94.
7. Zhu, J.; Li, R.; Niu, W.; Wu, Y.; Gou, X.; *Int. J. Hydrogen Energy*, **2013,** *38*, 10864.
8. Durano, M.; Tamboli, A.; Kim, H.; *Colloids Surf. A,* **2017,** 520,355.
9. Tomboc, G.; Tamboli, A.; Kim, H.; *Energy*, **2017**, *121*, 238.
10. Xie, L.; Wang, K.; Du, G.; Asiri, A.; Sun, X.; *RSC Adv.*, **2016**, *6*, 88846.
11. Wang, J.; Ke, D.; Li, Y.; Zhang, H.; Wang, C.; Zhao, X.; Yuan, Y.; Han, S.; *Mater. Res. Bull.*, **2017**, *95*, 204.
12. Wang, H.; Zhao, Y.; Cheng, F.; Tao, Z.; Chen, J.; *Catal. Sci. Technol.*, **2016**, 6, 3443.
13. Marchionni, A.; Bevilacqua, M.; Filippi, J.; Folliero, M.; Innocenti, M.; Lavacchi, A.; Miller, H.; Pagliaro, M.; Vizza, F.; *J. Power Sources*, **2015**, *299*,391.
14. Sukachiene, Z.; Tamasauskaite, L.; Jasulaitiene, V.; Bakiunaite, A.; Naujokaitis, A.; Norkus, E.; *Thin Solid Films*, **2017**, *636*,425.
15. Li, H.; Liao, J.; Zhang, X.; Liao, W.; Wen, L.; Yang, J.; Wang, H.; Wang, R.; *J. Power Sources*, **2013**, *239*,277.
16. Paladini, M.; Arzac, G.; Godinho, V.; Haro, M.; Fernandez, A.; *Appl. Catal. B-Environ.*, **2014**, *158*,400.
17. Jadhav, H.; Suryawanshi, S.; More, M.; Sinha, S.; *J. Alloys Compd.*, **2018**, *744*, 281.
18. Zanchetta, C.; Patton, B.; Guella, G.; Miotello, A.; *Meas. Sci. Technol.*, **2007**, *18*, N21.
19. Edla, R.; Patel, N.; Orlandi, M.; Bazzanella, N.; Bello, V.; Maurizio, C.; Mattei, G.; Mazzoldi, P.; Miotello, A.; *Appl. Catal. B-Environ.*, **2015**, *166*, 475.
20. Chlebda, D.; Jedrzejczyk, R.; Jodlowski, P.; Lojewska, J.; *J. Raman Spectroscopy*, **2017**, *48*, 1871.
21. Pfeil, T.; Pourpoint, T.; Groven, L.; *Int. J. Hydrogen Energy*, **2014**, *39*, 2149.
22. Mahmood, J.; Jung, S.; Kim, S.; Park, J.; Yoo, J.; Baek, J.; *J. Mater. Chem.*, **2015**, *27*, 4860.
23. Nandi, D.; Manna, J.; Dhara, A.; Sharma, P.; Sarkar, S.; *J. Vac. Sci. Technol. A*, **2016**, *34*, 01A115.
24. Edla, R.; Gupta, S.; Patel, N.; Bazzanella, N.; Fernandes, R.; Kothari, D.C.; Miotello, A.; *Appl. Catal. A-Gen.*, **2016**, *515*, 1.
25. Choi, S.; Lapitan, L.; Cheng, Y.; Watanabe, T.; *Adv. Power Technol.*, **2014**, *25*, 365.